FTIR-Spectroscopy of Multistranded Coiled Coil Proteins

Thomas Heimburg,*,‡ Juergen Schünemann,§ Klaus Weber,§ and Norbert Geisler*,§

Max Planck Institute for Biophysical Chemistry Departments of Spectroscopy and Biochemistry D-37018 Goettingen, Federal Republic of Germany

Received December 30, 1998; Revised Manuscript Received July 20, 1999

ABSTRACT: Coiled coils of different order were investigated using infrared (IR) spectroscopy. Recently, we demonstrated that dimeric coiled coils display unique vibrational spectra with at least three separable bands instead of only one band of a classical α-helix in the amide I region.This was attributed to a distortion of the helical structure by the supercoil bending, giving rise to bands that are not observed in the undistorted helix. Here, we investigated coiled coils forming trimers, tetramers, and pentamers. These higher order coiled coils, in general, possess larger superhelical pitches, resulting in a smaller helical distortion. We found that all coiled coils studied, including the native dimeric GCN4 leucine zipper and its variants leading to parallel trimers and tetramers as well as the rod portions of fibritin (parallel trimer), α-actinin (antiparallel spectrin type trimer), and COMP (parallel pentamer), displayed the typical three band pattern of the coiled coil amide I spectra. However, the separation of these three bands and their positional deviation from the classical α-helical band position was correlated to the extent of the helical distortion as reflected by the pitch values of the supercoils. The most pronounced spectral anomaly was found for the tropomyosin dimer with a reported helical pitch of 137 Å, whereas the smallest spectral distortion was found for the pentameric COMP complex and the tetrameric leucine zipper mutant, both with a pitch of about 205 Å.

Coiled coils are important oligomerization elements of proteins. They are built from α-helices carrying a seven-residue repeat pattern (*a* to *g*) of hydrophobic and hydrophilic residues in which the hydrophobic residues occupy the first (*a*) and the fourth (*d*) positions (*1*). This generates a hydrophobic seam along the axis of the helix along which two or more helices align laterally in parallel or antiparallel fashion. The tight contact of neighboring helices is achieved by a "knobs into holes" arrangement of the hydrophobic residues in the interface (*2*). Additional stabilization of the dimer and the correct positioning with respect to register arises from ionic interactions of residues close to the interface. The "classical" form of a coiled coil is double-stranded, parallel, and in register and involves two identical chains. However, there are many other forms of coiled coils. They differ with respect to chain number and orientation and can be homo- as well as heterotypic.

The fixed number of two hydrophobic residues in the seven-residue-long repeat unit, (i.e., one hydrophobic residue per 3.5 residues) resulting in an amphiphatic helix versus the slightly higher number of around 3.65 residues per turn of straight α-helix, leads to a left-handed axial shift of the hydrophobic seam around the helix. As a consequence, coiled coils display a distinct left-handed twist. Its pitch length will depend on several factors such as the primary sequence, i.e., the actual choice of hydrophilic and hydrophobic residues within the repeat units. This can result in local variations of the pitch length in distinct regions of a coiled coil (see, e.g., refs *3*−*6*, for tropomyosin). Other important factors for the characterization of a coiled coil include the radius of curvature, the diameter, the number of helices it contains, and the crossing angle of the helices. In addition, coiled coils are not always continuous over their entire length. Instead, the regular repeat pattern can be segmented by stutters or by short outlooping sequences, allowing each shorter segment to adopt its own pitch (e.g., see fibritin (*7*)).

The repeat structure of the coiled coil results in helix bending and a regular axially repeated distortion of the hydrogen bonds. The bond angles are changed, and their lengths are shortened in the inner side, i.e., close to the hydrophobic seam, and lengthened at the outer side (e.g., ref *8*, for an atomic structure of a dimeric coiled coil). The resulting distortions of the usual vibrational characteristics of the participating atomic moieties (backbone C═O and N−H) can be monitored by infrared spectroscopy. Recently, we reported the Fourier transform infrared (FTIR) spectra observed with classical double-stranded coiled coils, such as tropomyosin and the rod domains of myosin and of the intermediate filament proteins desmin and vimentin (*9*). We demonstrated a strong deviation of the coiled coil spectra in the amide I region from that of the classical α-helix. Instead of a single peak, the coiled coil spectra are composed of three peaks that probably represent the three vibrational modes of α-helices (A, E1, and E2; ref *10*). These are all IR-active due to the absence of translational symmetry. Two of the three bands were found at significantly lower wavenumber than the α-helical bands.

Here, we report the FTIR-spectra of several multistranded coiled coils. These include the native dimeric GCN4 leucine

* To whom correspondence should be addressed. T.H.: Telephone, +49-551-201 1491; fax, +49-551-201 1501; E-mail, theimbu@gwdg.de. N. G.: Telephone, +49-551-201 1486; fax, +49-551-201 1578. Max Planck Institute for Biophysical Chemistry, P.O. Box 2841, D-37018 Goettingen, Federal Republic of Germany.

‡ Department of Spectroscopy.

§ Department of Biochemistry.

10.1021/bi983079h CCC: $18.00
Published on Web 09/08/1999

zipper (*8*) and its permutational leucine/isoleucine variations in the *a*- and *d*-positions leading from dimers to parallel trimers and tetramers (*11*). Other multichain coiled coils investigated here are T4 fibritin, a parallel trimer (*7*, *12*), and the rod domains of α-actinin; which contains antiparallel spectrin-type trimeric units (for a review, see ref *13*, *14*), and of COMP, a parallel pentameric coiled coil domain (*15*, *16*).

MATERIALS AND METHODS

Coiled Coils: A set of GCN4 peptides (GCN4-p1, GCN4-p1IL, GCN4-p1II, GCN4-p1LI, GCN4-p1s, GCN4-p1ILs, GCN4-p1IIs, and GCN4-p1LIs, for primary sequences, see below) were provided by Drs. Jürgen Wehland and Dr. Ronald Frank (Gesellschaft für biotechnologische Forschung GBF, Braunschweig, Germany). They were purified by RP-HPLC and characterized by primary sequence and mass. Their primary sequences were chosen according to (*17*) and are based on the data presented by (*11*). Peptides with index "s" are shorter by one residue at the N-terminus and at the C-terminus than the authentic leucine zipper sequence, which comprises the C-terminal 33 residues of the GCN4 protein with an acetylated N-terminus (GCN4-p1, supplied by Dr.Anton Karabinos, Göttingen). The GCN4-p1 peptide was, in addition to the *N*-acetylation, C-amidated, while the GCN4-p1I/L peptides were N− acetylated but not C-amidated (as in ref *8*). In addition, the C-terminal residue of the shorter peptides was changed from E (authentic) to Q. The primary sequences are:

GCN4-p1 dimer
Ac−RMKQLEDKVEELLSKNYHLENEVARLKKLV-GER−$CONH_2$

GCN4-p1IL dimer
- - - -L- - -I- -L- - -I- -L- - -I- -L- - -I- - -

GCN4-p1II trimer
- - - -I- - -I- -I- - -I- -I- - -I- -I- - -I- - -

GCN4-p1LI tetramer
- - - -I- - -L- -I- - -L- -I- - -L- -I- - -L- - -

GCN4-p1s dimer
MKQLEDKVEELLSKNYHLENEVARLKKLVGQ

GCN4-p1ILs dimer
- - -L- - -I- -L- - -I- -L- - -I- -L- - -I- -

GCN4-p1IIs trimer
- - -I- - -I- -I- - -I- -I- - -I- -I- - -I- -

GCN4-p1LIs tetramer
- - -I- - -L- -I- - -L- -I- - -L- -I- - -L- -

Turkey α-actinin was supplied by Manfred Ruediger (University of Braunschweig, Germany). The rod domain covering repeats 1−4 was prepared by thermolytic digestion of the intact protein (*18*) and purified by chromatography on MonoQ resin according to ref *19*. It comprises residues 266 to 714 of the corresponding chicken sequence (reviewed in ref *14*).

Recombinant full-length T4 fibritin (*12*) was supplied by Vadim Mesyanzhinov (Moskau, GUS). Recombinant rod from rat COMP (cartilage oligomeric matrix protein; (*15*)) comprising residues 20 to 83 was supplied by Dr. Juergen Engel (Basel, Switzerland). Bovine skeletal muscle tropomyosin was purified as described (*20*). Coiled coils were prepared for FTIR-spectroscopy by extensive dialysis against D_2O buffers at concentrations of 2−10 mg/mL at ambient temperature with at least two buffer changes (buffer volume 20 mL; sample volume 100 μL). Specific buffers used for dialysis were: (1) 50 mM potassium phosphate buffer, pD 7.0, 150 mM NaCl (GCN4 peptides); (2) 50 mM sodium phosphate buffer, pD 8.0, 200 mM NaCl (COMP); (3) 50 mM Tris-HCl buffer, pD 7.5 (fibritin); (4) 20 mM Tris-HCl, pD 7.6, 20 mM NaCl (α-actinin rod); (5) 10 mM Tris-HCl, pD 7.5, 170 mM NaCl, 1 mM 2-mercaptoethanol (tropomyosin); (6) 50 mM potassium phosphate buffer, pD 7.0, 150 mM NaCl, 1 mM 2-mercaptoethanol (c-Fos peptide).

FTIR-Spectroscopy: FTIR-spectroscopy was performed on a Bruker IFS25 spectrometer using a CaF_2 cell with a Teflon spacer (50 mm). The spectra (100 interferograms) were obtained in the range 400−4000 cm^{-1} with a spectral resolution of 2 cm^{-1}. Spectra were apodized with a triangular function before Fourier transformation. Fourier self-deconvolution was performed with software using routines provided by the laboratory of Dr. H. H. Mantsch/Ottawa (*21*, *22*). Resolution enhancement of unsmoothed spectra was performed using a triangular apodization function and line narrowing factors between 1.0 and 2.0. The initial line width was assumed to be Lorentzian with a line width of 17 cm^{-1}. The spectral components of the resolution enhanced spectra were fitted with bands of Gaussian line shape (*23*). Spectra were recorded at room temperature. The deuterium exchange was found to be complete in each case.To avoid interference with amino acid side chain vibrations, the absorbance of these bands was subtracted (*24*−*26*). The side chain absorbance was composed from the bands of Asp, Glu, Asn, Gln, Tyr, Arg, and $C_\alpha OO^-$ (given by ref *24*), according to their frequency in the primary sequence. In the case of bovine skeletal tropomyosin, where we did not know the primary sequence, we instead subtracted the side chain contributions of rabbit cardiac muscle tropomyosin.

RESULTS

Recent results on the dimeric coiled coil proteins tropomyosin, myosin rod, and desmin rod (*9*, *10*) suggested that the supercoil bending of the α-helices results in a spectral splitting of the α-helical IR amide 1 band and in a shift to lower wavenumbers due to bifurcated hydrogen bond formation with the solvent (for a split hydrogen bond at the outer side of a bent amphiphilic helix see ref *27*. Here, we have investigated by FTIR a variety of proteins or protein domains forming coiled coils with strand numbers ranging from 2 to 5 (dimers to pentamers), for which high-resolution X-ray and, in some instances, NMR structures are available (*28*, *29*). One characteristic feature of a coiled coil deducible from high-resolution structures is the superhelical pitch, which is the length of the axial periodicity of the coiling (listed in Table 1). Our analysis emphazises the relationship between the α-helical amide I IR spectra and the pitch values of the different dimeric and multistranded coiled coils.

Table 1: Band Positions and Areas of the Amide I Spectra of the Investigated Coiled Coils

	band 1 (cm^{-1})	band 2 (cm^{-1})	band 3 (cm^{-1})	band 4 (cm^{-1})	band 5 (cm^{-1})	spectral weight [cm^{-1}]	spectral max. [cm^{-1}]	superhelical pitch [Å]
tropomyosin	1607	1626	1639	1652	1668	1638.7	1636.6	137 (ref 5)
	(7.9)	(24.9)	(33.0)	(23.9)	(10.3)			
GCN4-p1 leucine zipper	1606	1631	1641	1651	1672	1640.9	1640.5	147.6 (ref 11)
	(2.7)	(40.8)	(10.7)	(37.1)	(8.7)			
GCN4-p11L	1606	1631	1642	1651	1669	1640.9	1642.7	147.6 (ref 11)
	(5.6)	(30.9)	(27.2)	(27.3)	(9.0)			
GCN4-p11I	1614	1631	1641	1651	1668	1642.1	1643.8	175 (ref 46)
	(7.2)	(25.6)	(20.2)	(34.3)	(12.6)			
GCN4-p1LI	1615	1631	1642	1651	1666	1642.3	1645.4	205.4 (ref 11)
	(8.2)	(24.2)	(19.4)	(31.9)	(16.3)			
fos leucine zipper (monomer)	1621	1630	1640	1651	1668	1643.7	1643.0	
	(9.3)	(15.2)	(17.5)	(37.5)	(20.6)			
a-actinin rod	1614	1629	1640	1650	1672	1644.1	1647.6	(187, ref 29)
	(5.4)	(11.7)	(23.8)	(46.8)	(12.3)			
COMP rod	1600	1631	1644	1652	1673	1644.6	1647.1	204 (ref 16)
	(1.2)	(25.0)	(17.9)	(47.9)	(8.0)			
fibritin	1610	1631	1641	1651	1670	1642.6	1643.7	(137.8, ref 8)
	(6.3)	(21.2)	(20.6)	(35.0)	(16.7)			
hemoglobin	1621		1638	1656	1675	1649.1	1653.8	∞
	(8.9)		(30.7)	(48.4)	(12.0)			

[a] Deduced from the band positions are the spectral weights, (ν), calculated from the three large central peaks [$(\nu) = (a\nu_a + b\nu_b + c\nu_c)/(a + b + c)$]. Spectral maxima are those of the un-deconvolved amide I band. Pitch values were taken from the literature as indicated in the last column. The pitch lengths, set in parentheses, were determined for related proteins or fragments. The α-actinin pitch value is averaged from the three separate values for the structurally related R16 unit of chicken brain α-spectrin, and the fibritin pitch length was obtained as an average of three out of twelve coiled coil segments (see also text and Materials and Methods). Band positions were rounded to integer values. The spectral maxima and weigths are given with higher resolution.

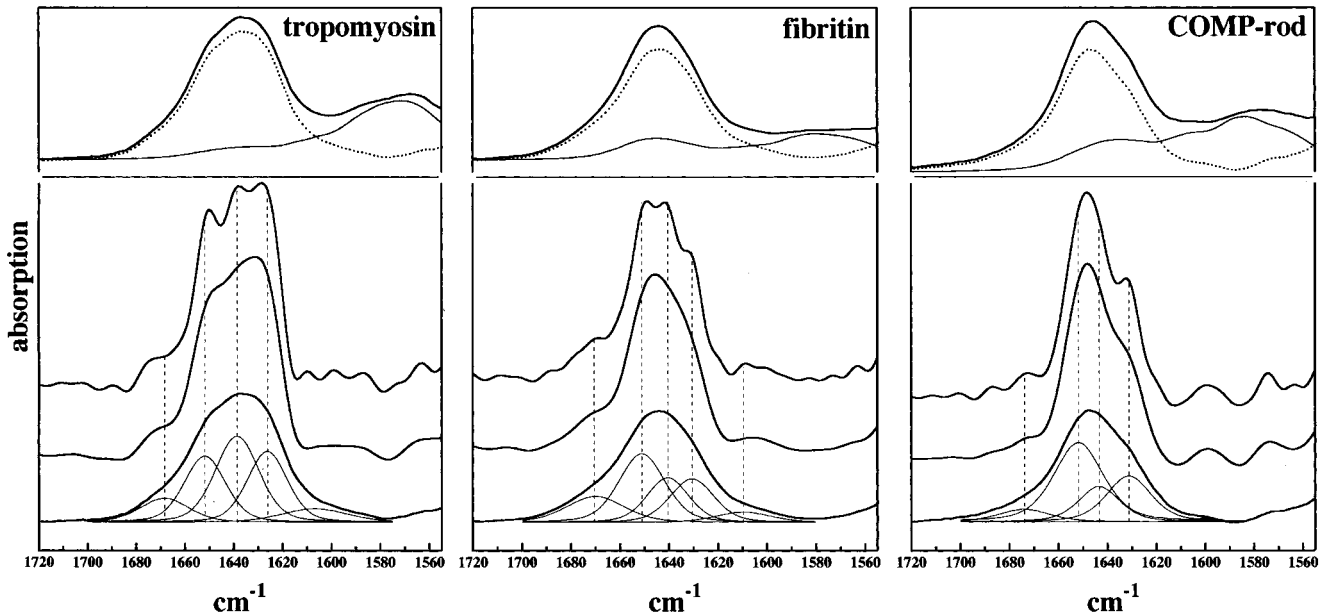

FIGURE 1: Band decomposition of the amide I region of tropomyosin (A, double-stranded), fibritin (B, parallel triple-stranded) and COMP (C, parallel pentameric). The top panels indicate the subtraction procedure of side chain contributions (*24*). In the bottom panels, the subtracted spectra were deconvolved with three different line narrowing factors of $K = 1$ (bottom, original spectrum), 1.5 (middle), and 2 (top), using an intrinsic line width of 17 cm^{-1}. Band positions were obtained by fitting the resolution enhanced spectra at the top. These positions were used to fit the original spectra.

Figure 1 displays the amide I spectra of three representative coiled coil proteins or coiled coil domains with increasing numbers of parallel helices. Tropomyosin (A) is the classical representative of a parallel dimeric coiled coil. The fingerprint pattern of the three major bands has been described previously (*9*). The spectrum of fibritin, which forms a parallel trimeric coiled coil, is shown in (B), and the spectrum of the pentameric COMP-rod is shown in (C). In the top panels, the subtraction procedure for the side chain contributions to the infrared absorbance is given (*24*−*26*). In the bottom panels, the amide I spectra of the protein backbone are given at three different resolution enhancement factors ($K = 1$, $K = 1.5$, and $K = 2.0$) as obtained by spectral Fourier deconvolution (*21*, *22*). The spectrum with the most pronounced resolution enhancement was fitted with a band fitting routine. The band positions of the three fingerprint bands obtained in these fits were then used to fit the original spectra, which contain less pronounced features. It is obvious from Figure 1, B and C, that the trimeric coiled coil also displays a three band pattern. In analogy with the other coiled coil spectra, the pentameric coiled coil has also been fitted with a three line pattern, although the two bands at higher

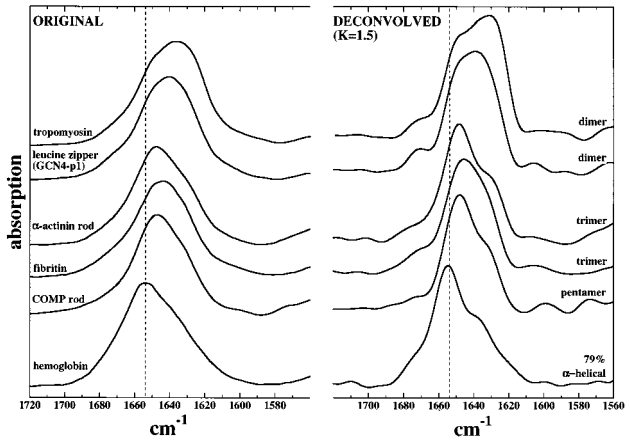

FIGURE 2: Infrared spectra of different coiled coil proteins forming dimers, trimers, tetramers, and pentamers after subtraction of side chain contributions. The original spectra are given in the left panel and slightly resolution enhanced spectra (factor = 1.5 and an intrinsic line width of 17 cm^{-1}) in the right panel. The spectra were ordered, according to the helical pitch, with the dimeric tropomyosin at the top (pitch = 137 Å) and the pentameric COMP-rod at the bottom (pitch = 205 Å). This order also reflects the strandedness of the coiled coils. The spectrum of hemoglobin, which is a highly helical protein but does not contain supercoils is displayed at the bottom for comparison. The dotted line indicates the classical α-helical band position (30).

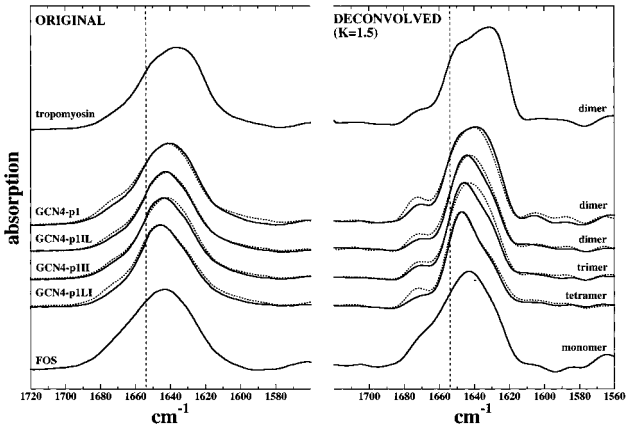

FIGURE 3: Infrared spectra of the GCN4-p1 leucine zipper and of some of its mutants, compared to tropomyosin after subtraction of side chain contributions. The original spectra are given in the left panel and slightly resolution enhanced spectra (factor = 1.5 and an intrinsic line width of 17 cm^{-1}) in the right panel.. Whereas the authentic GCN4 leucine zipper dimer (GCN4-p1) displays a spectrum and a pitch comparable to tropomyosin, the tetrameric mutant with a pitch of about 205 Å (GCN4-p1LI) displays a pronounced spectral shift to higher wavenumbers, indicating a reduced spectral and helical distortion. The other mutants, i.e., the GCN4 trimer (GCN4-p1II) are situated between the two extreme versions. Dotted curves represent the short versions of the GCN4-p1 mutants. They are comparable with the original peptides with the exeption of the GCN4-p1IIs peptide, which is distinctively different from the GCN4-p1II mutant. This indicates that the terminal amino acids may also be relevant for the tertiary structure.

wavenumbers could not clearly be separated in the deconvolved spectrum. This assumption, however, is not essential for the further data analysis. The shift of the three bands with respect to the classical α-helical band position at 1650−1653 cm^{-1} in D_2O (*30*) is for both, the trimeric and the pentameric coiled coil, smaller than in tropomyosin (Figure 1A) and the separation of the bands is less pronounced. Thus, although spectral anomalies are seen in the amide I spectrum of all three proteins, the spectra of the trimeric and pentameric proteins are closer to the undistorted helix and the spectra of tropomyosin show the highest deviation from an α-helical spectrum. The results of the detailed band fitting analysis of all proteins studied are summarized in Table 1. To quantify the spectral changes, the spectral weight center of the three major bands of the amide I region were calculated and the absorption maxima determined. Contrary to all coiled coil proteins analyzed, hemoglobin—a protein of high helical content but without supercoiling—displays a spectral weight close to the reported classical α-helical band position (Table 1).

Figure 2 compares the spectra of several different coiled coil proteins after subtraction of side chain contributions. The spectra are given both as raw data (left panel) and slightly resolution enhanced with a deconvolution factor of $K = 1.5$ and an intrinsic line width of 17 cm^{-1} (right panel). The figure contains spectra of the dimeric tropomyosin, the dimeric leucine zipper, the antiparallel triple-stranded α-actinin rod containing four spectrin-type units built from a single continuous but twice folded back α-helix, the parallel triple-stranded fibritin, and the parallel five stranded rod of COMP. The five coiled coil proteins are arranged in order of their pitch values. The spectrum of hemoglobin (Figure 2, bottom) represents a protein of high α-helical content with a close to infinite superhelical pitch (no helical distortion). From the data in Figure 2, it appears that a longer pitch results in a spectral center and a spectral maximum shifted to higher wavenumbers, and thus being closer to the classical α-helical amide I band position (1651 cm^{-1} in heavy water), which is represented by the strongest band in the spectum of hemoglobin.

Figure 3 presents a comparison of variants of the GCN4 leucine zipper, with the raw data (after subtraction of side chain contributions) in the left panel and the deconvolved spectra in the right panel. The GCN4 leucine zipper has a comparatively short length of 33 residues (*8*). However, it is generally considered as the prototype motive of a dimeric coiled coil, and its higher order variants serve as models for parallel trimeric and tetrameric coiled coils (*11*).

The leucine zipper dimer with the authentic sequence (GCN4-p1) has a pitch of 148 Å (*8*, *11*, *31*). This value is slightly higher than the 137 Å pitch of tropomyosin (*5*, *6*), judged by the crystal structures. However, the value for the leucine zipper may be somewhat variable, since it contains only about a third of one superhelical turn. The amide I spectra of tropomyosin and the dimer zippers are quite similar, although the leucine zipper spectrum is slightly shifted to higher wavenumbers, in agreement with the slightly higher superhelical pitch (for details see below).

In addition, we recorded a series of spectra of GCN4 leucine zipper mutants (see Materials and Methods): (i) GCN4-p1, authentic sequence, and a dimer; (ii) GCN4-p1IL, isoleucines in *a*-positions, leucines in *d*-positions, and a dimer; (iii) GCN4-p1II, isoleucines in *a*- and *d*-positions, and a parallel trimer with a pitch of 170 Å length (*31*); and (iiii) GCN4-p1LI, leucines in *a*-positions, and isoleucines in *d*-positions, and a parallel tetramer with a 205 Å long pitch (*11*, *31*). The two dimer variants (GCN4-p1 and GCN4-p1IL) yielded spectra similar to that of the longer, native zipper variant GCN4-p1. The trimer (GCN4-p1II) and the tetramer (GCN4-p1LI) with the 205 Å long pitch yielded a

spectrum nearly identical to that of the pentameric COMP-rod (204 Å pitch length, 16), suggesting a similar relatively small helical distortion.

Additionally, we investigated variants of the previous four peptides (GCN4-p1s, GCN4-p1ILs, GCN4-p1IIs, and GCN4-p1LIs), which lack two amino acid residues in the terminal regions of the peptide but are similar in sequence otherwise (see Materials and Methods). The spectra of these variants are given in Figure 3 as dashed lines, superimposing the mutants of original length. While the spectra of GCN4-p1 and GCN4-p1 (dimeric), GCN4-p1IL and GCN4-p1ILs (dimeric), and GCN4-p1LI and GCN4-p1LIs (tetrameric) are comparable, the spectra of GCN4-p1II (trimeric) and GCN4-p1IIs are different. The latter spectrum resembles that of the dimeric peptides. It is likely, therefore, that GCN4-p1IIs in contrast to the trimeric coiled coil GCN4-p1II forms a dimer. This indicates that the terminal amino acids contribute to the tertiary structure of the peptides.

The change in the spectra of the 3 GCN4-p1 mutants peptides (GCN4-p1ILs, GCN4-p1II, and GCN4-p1LI) is especially interesting since they have the same composition of side chains that absorb in the amide I region. Nevertheless, the spectra are distinctly different. This rules out that side chain absorption is responsible for spectral shifts.

The zipper peptide of the c-Fos oncogen protein also yielded a spectrum similar to the GCN4 zipper dimer (Figure 3). However, this peptide does not form homotypic coiled coils (*32*) and thus should be considered to be a monomer. Possibly even this monomer can adopt structural characteristics (bending and twist) of coiled coil proteins (see Discussion).

One aim of our study was to see whether there is a relation between the superhelical pitch and the infrared spectra of coiled coils. The distortion of IR-spectra is expected to be correlated to the mean curvature per amino acid in an α-helix. As long as the pitch is much longer than the diameter of of a multimeric coiled coil, it is approximately proportional to the number of residues in one full superhelical turn. This implies that the inverse, i.e., 1/pitch, is roughly proportional to the mean curvature per residue, expressed as fraction of one turn. The larger the 1/pitch value the larger is the helical curvature, which in turn is equivalent to the distortion of the helical parameters as discussed above (i.e., for example, the lengthening and shortening of hydrogen bonds).

Figure 4 summarizes the analysis. It compares the inverse of the superhelical pitch with the shift of the amide I spectral weight center toward lower wavenumbers. The inverse pitch length is clearly correlated with the position of the amide I spectral weight, and consequently with the helical distortion, i.e., the shorter the pitch length the higher the distortion (see the insert of Figure 4). This correlation was also detected in the spectral maxima of the un-deconvolved protein spectra (after subtraction of side chain contributions) versus the inverse pitch length and is, therefore, neither dependent on the deconvolution procedure nor on the different side chain composition of the proteins. All coiled coils fall roughly into two groups with only small differences in each group: (i) all dimers, and (ii) all multichain coiled coils beyond the dimer, i.e., from trimers to pentamers have similar spectral center points. Both groups are distinctly separated from straight α-helices such as those in hemoglobin and myoglobin [79% helical, (*33*; Figures 2−4; Table 1].

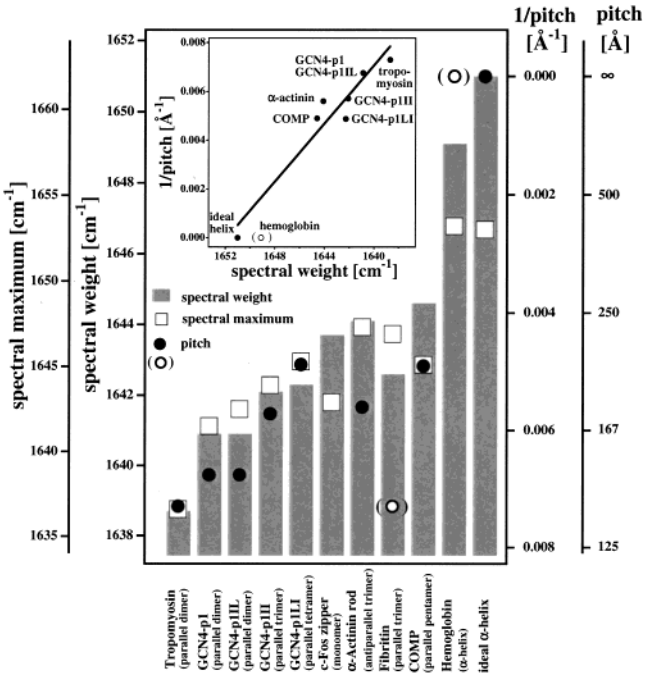

FIGURE 4: Correlation of the inverse of the helical pitch (1/pitch) as a linear measure for the helical curvature and distortion with the spectral weight (and the spectral maximum) of the α-helical amide I spectra of the different proteins listed in Table 1. A nonlinear axis showing the unreversed pitch length is added at the side for easier orientation. The general dependence of the spectral weight on the pitch is obvious. The pitch of fibritin is exceptional low relative to its spectral center position and the c-Fos leucine zipper peptide is most likely monomeric and hence its supercoil pitch is unknown (see text for possible explanations). There is no authentic pitch value available for the antiparallel trimer coiled coil of the α-actinin rods. Instead, the average of the three dimer pitch values reported for the solution structure of the R16 triple helix repeat of chicken spectrin brain α-spectrin (*29*) is used. The helices in hemoglobin are considered to be mostly straight. Since exact values for its helical distortion were not available, the classical α-helical band position with zero distortion as reference point is included. The pitch values were taken (i) for tropomyosin from (*4*−*6*); (ii) for GCN4 leucine zippers from (*8*, *11*, *46*); (iii) for the spectrin-type repeat unit from (*29*); (iv) for the rod from COMP from (*16*); (v) for fibritin from (*7*). The insert demonstrates the coupling of the spectral weight with the helical pitch.

The spectrum of the trimeric coiled coil of fibritin indicates, however, less helical distortion than expected from the low pitch length of 138 Å (averaged pitch values of the three C-terminal segments) (*7*). The 53-nm-long rod of fibritin is an example for a segmented coiled coil where short nonhelical streches loop out and allow for different pitch values in each segment. The rod, which comprises about 80% of the entire fibritin sequence, is segmented into approximately 12 segments. The recent X-ray diffraction structure of the C-terminal three segments (*7*) shows that their pitch values are 110, 139, and 165 Å respectively. Thus, there is a high heterogeneity of the helical parameters. In addition the averaged pitch value of 138 Å relates only to about one-fourth of the entire molecule. Thus, the observed deviation of the fibritin spectrum from the general scheme (see above) may be related to the unique features of fibritin.

For the antiparallel spectrin-type triple helix of the α-actinin rod, no atomic resolution data are available. Therefore, we used the recently published solution structure of the related R16 repeat unit of α-spectrin to calculate an average pitch value using the three different values given

for each possible pair of the triplet (*29*). The difference of the three pitch values (198, 157, and 180 Å) indicates that the unit is distinctly asymmetrical and, therefore, not a "perfect" example for an antiparallel triple helix.

Finally, it should be noted that the relation of the inverse pitch value with the spectral weight is also evident when the amide I band maximum is used (Table 1). The longer the reported pitch the closer is the band maximum to the known α-helical band position at 1651 cm^{-1}.

DISCUSSION

Amide I infrared spectra of several dimeric, trimeric, tetrameric, and pentameric coiled coils were recorded. All exhibit a significant spectral deviation from the classical α-helix, most of them with the typical triplet characteristics of coiled coil spectra first recognized for the dimeric coiled coils of tropomyosin, and of the myosin and desmin rods (*9*). This type of spectrum is thought to indicate distortions of the helical parameters, such as hydrogen bond angles and lengths as well as bifurcation and interaction with water molecules as displayed in the stereoview in Blundell et al. (*27*). The reason for these distortions are likely to be found in the supercoil bending of the helices in the coiled coil. The three major bands probably represent the three vibrational modes of α-helices (A, E1, and E2) (*10*). The absolute positions of these three bands, according to Reisdorf and Krimm (*10*), depend on details of the hydrogen bonding patterns to adjacent amino acids and to the solvent. In their theoretical study on topomyosin, it was not attempted to assign the three fingerprint bands to any of the three vibrational modes. In a straight α-helix, however, the E2-mode is not IR-active due to the translational symmetry of the helix. The amplitude of this band is, therefore, expected to increase with progressive bending of the helix. Thus, the intensity of the bands reflects the degree of symmetry breaking, whereas the band positions reflect the corresponding hydrogen bonding patterns with adjacent carbonyl groups and with water.

In a simplified view, the pitch of the supercoil bending is related to the number of helices constituting the coiled coil. The lowest pitch values (around 137 Å), and consequently, the strongest distortion of helical parameters, is found in double-stranded coiled coils such as tropomyosin or in the dimeric leucine zippers, while the highest values, and the least distortion, is found with multimeric coiled coils, such as in the pentameric COMP-rod (around 204 Å). An exeption to this rule is the extremely short pitch (109 Å) of the central triple-stranded coiled coil section of the fibritin fragment analyzed by X-ray crystallography (*7*). Furthermore, a recent study with a single mutant in the GCN4 leucine zipper (*31*) showed that already very subtle sequence changes can lead to strong changes in the properties of the coiled coil: the occurrence of the mutated zipper in both a dimer and a trimer form, accompanied by an increase of the helix crossing angle and a reduction of the pitch value in the trimer versus the dimer. Thus, the helical parameters, including pitch values, appear to relate not only to the number of helices but also can vary significantly depending on subtle sequence changes.

Despite these difficulties, most coiled coil spectra exhibit a distinct coordination with the pitch values. An exception to this may be the fibritin trimer as outlined above (see Figure 4; Table 1). However, the true avarage pitch for the whole fibritin rod may be higher than the one used here, which represents the average value for only three out of 12 rod units for which the structure at atomic resolution is known ((*7*), see above).

In addition to the GCN4 leucine zippers, we recorded spectra from the c-Fos oncogene zipper (*32*) under conditions identical to those used for the GCN4 zippers. Interestingly, the c-Fos zipper peptide, which does not form homotypic coiled coils and is thought to be monomeric without the jun protein (*32*) yielded spectra similar to the GCN4 dimer zipper and to tropomyosin (Figure 3). If it is true that the c-Fos zipper peptide does not form homotypic dimers in significant amounts under the conditions used, i.e., high concentration at pH 7.0, then our results indicate that already the monomeric c-Fos α-helix is similarly distorted in its helical parameters and has a superhelical twisting as if it were situated in a coiled coil (i.e., the heterotypic dimer with a Jun oncogen zipper helix peptide (*32*)). A possible reason for this could be that axial sequence periodicities along an α-helix may cause helix bending. Thus, amphipatic α-helices in proteins often appear to be bent with the hydrophobic residues in the inner convex side and the hydrophilic residues at the outer concave side (*27*). Pauling and Corey (*34*) first suggested that the curvature of α-helices could be caused by a difference in the hydrogen bond lengths at inner and outer sides. More recent structural data at atomic resolution (8, *35*) as well as independent NMR results on hydrogen exchange rates (*36*) confirm that the reason for supercoiling is the occurrence of shorter and longer hydrogen bond distances along the α-helices with a periodicity matching the seven-residue coiled coil repeat structure. As is the case with the seven-residue coiled coil repeat, the hydrophobic seam shifts axially around the helix, possibly causing even the monomeric c-Fos zipper α-helix to adopt a superhelically twisted structure, which in turn may give rise to its coiled coil type spectrum.

The IR spectra of tropomyosin given here and previously (*9*) were obtained in D_2O buffer. Venyaminov and Kalnin (*26*) analyzed tropomyosin (rabbit skeletal muscle) in H_2O. In their un-deconvolved data, a three-line pattern was not obvious. Instead, the authors fitted the amide I absorbance by one single band. However, as in our data, the position of this band (1647 cm^{-1}) is found at a significantly lower wavenumber than the classical position of an α-helix in H_2O at 1658 cm^{-1}. Furthermore, their overall band halfwidth (33 cm^{-1}) is comparable to that found here in D_2O (~25 cm^{-1}). The reason for the absence of an obvious three-line pattern of tropomyosin in H_2O may be caused by the hydrogen bonds to the solvent, which are of different strength in D_2O and H_2O. A difference of helical band positions was also found for calmodulin in D_2O and H_2O (*37*, *38*) and is discussed below.

The results reported here are interesting in respect to the general deduction of secondary structure from protein amide I spectra. To assign bands, it is usually assumed that the alignment of hydrogen bonds and their strength is constant for a given structural feature, therefore, resulting in well-defined band positions for specific secondary structure elements. Our data, however, suggest that in curved helices this is not generally the case. Reisdorf and Krimm (*10*) argued that the symmetry breaking in bending a helix results

in infrared activity of the three principle vibrational modes (A, E1, and E2). Heimburg et al. (*9*) suggested that coiled coil proteins (or curved helices in general, see also (*27, 39*)) possess bifurcated hydrogen bonds both to adjacent amino acid residues and to the solvent, thus affecting the overall hydrogen bonding strength of each residue. If this is the case, than the exact position of the three bands depends on the relative alignment and the number of hydrogen bonds. It is, therefore, likely that changes in band postions caused by stretching or bending of helices is solvent-dependent and different for D_2O (or H_2O) exposed helices and transmembrane helices.

Unusual positions of α-helical bands have already been reported. They were for example found in short helix segments (*40*). Bacteriorhodopsin has one band at the unusually high wavenumber of 1665 cm^{-1} (*41*). It was suggested that this is due to an unusual bend in one of the helices (*10*). According to (*42*), however, one helix seems to be stretched rather than curved, therefore, weakening the hydrogen bonding pattern and consequently resulting in a shift to higher wavenumbers. Nevertheless, bifurcated hydrogen bonding to solvent molecules is not possible in a transmembrane segment. Furthermore, unusually low-helical bands in calmodulin and troponin C around 1644 cm^{-1} (in D_2O) were assumed to be due to helix distortion (*37*). Interestingly, these unusual positions in the proteins were not found in H_2O buffer (*38*). In sarcoplasmic reticulum Ca^{2+}−ATPase, the helix position was assigned at 1645 cm^{-1}. Helical bands in calcinotin were assigned at 1637 cm^{-1} (*43*) and in alanin-based peptides as low as 1632−1635 cm^{-1} (*44*). In the same spectral region, α-helical bands (additional to bands at the classical position) of apolipoprotein fragments have been proposed (*45*). As in our previous study (*9*), the authors suggest bifurcated hydrogen bonds as a possible explanation (*45*). Finally, it may be possible that even in hemoglobin some helical segments are distorted. A spectrum with at least two pronounced bands has been found where the sum of the band areas corresponds to to overall helical content of this protein. However, the spectral shifts are much smaller as in the coiled coils.

Our results confirm and extend the notion that coiled coils display a α-helical amide I IR-spectrum distinct from that of the normal α-helix (*9*). The extent to which the coiled coil spectrum deviates from the normal spectrum correlates with the pitch value of the α-helices in the coiled coils: the deviation of the spectrum and thus the deformation of the helix, is strongest for dimeric coiled coils, and less strong for multimeric coiled coils. It remains to be seen whether bent α-helices of globular proteins, especially amphiphatic ones, display similar spectra, or if the spectra described in this study arise solely from coiled coils. However, some of the results in the literature, which are discussed above, suggest that this is the case. The coupling of the helical curvature with the band positions may represent a step to better understanding of amide I band positions.

ACKNOWLEDGMENT

We are indebted to Dr. Derek Marsh for support and use of infrared equipment. We thank Drs. Manfred Ruediger (Braunschweig), Jürgen Engel (Basel), and Vladim Mesianzhinov (Moscow) for providing proteins for this study. Drs. Ronald Frank and Jürgen Wehland (GBF, Braunschweig) provided the seven leucine zipper mutants, while Dr. Anton Karabinos (Göttingen) provided some of the GCN4 and c-Fos zipper peptides. We acknowledge correspondence with and helpful remarks of Drs. Murray Stewart (Cambridge), Yizhi Tao and Michael Rossmann (West Lafayette), Michael Nilges (Heidelberg), and Tom Alber (Berkeley).

REFERENCES

1. Heimburg, T., Schuenemann, J., Weber, K., and Geisler, N. (1996) *Biochemistry 35*, 1375−1382.
2. Sodek, J., Hodges, R. S., Smillie, L. B., and Jurasek, J. (1972) *Proc. Natl. Acad. Sci. U.S.A. 69*, 3800−3804.
3. Crick, F. H. C. (1953) *Acta Crystallogr. 6*, 689−697.
4. Parry, D. A. D. (1975) *Nature* (London) 256, 346−347.
5. McLachlan, A. D., andStewart, M. (1975) *J. Mol. Biol. 98*, 293−304.
6. Phillips, G. N., Jr., Fillers, J. P., and Cohen, C. (1986) *J. Mol. Biol. 192*, 111−131.
7. Whitby, F. G., Kent, H., Stewart, F., Stewart, M., Xie, X., Hatch, V., Cohen, C., and Phillips, Jr., G. N. (1992) *J. Mol. Biol. 227*, 441−452.
8. Tao, Y., Strelkov, S. V., Mesyanzhinov, V. V., and Rossmann, M. G. (1997) *Structure 5*, 789−798.
9. O'Shea, E. K., Klemm, J. D., Kim, P. S., and Alber, T. (1991) *Science 254*, 539−544.
10. Reisdorf, W. C., and Krimm, S. (1996) *Biochemistry 35*, 1383−1386.
11. Harbury, P. B., Zhang, T., Kim, P. S., and Alber, T. (1993) *Science 262*, 1401−1407.
12. Efimov, V. P., Nepluev, I. V., Sobolev, B. N., Zurabishvili, T. G., Schulthess, T., Lustig, A., Engel, J., Haener, M., Aebi, U., Venyaminov, S. Y. Potekhin, S. A., and Mesyanzhinov, V. (1994) *J. Mol. Biol. 242*, 470−486.
13. Parry, D. A. D., Dixon, W., and Cohen, C. (1992) *Biophys. J. 61*, 858−867.
14. Blanchard, A., Ohanian, V., and Critchley, D. R. (1989) *J. Muscle Res. Cell Motil. 10*, 280−289.
15. Efimov, V. P., Lustig, A., and Engel, J. (1994) *FEBS Lett. 343*, 54−58.
16. Malashkevich, V., Kammerer, R. A., Efimov, V. P., Schulthess, T., and Engel, J. (1996) *Science 274*, 761−765.
17. Delano, W. L., and Brünger, A. T. (1994) *Proteins: Struct. Funct. Gen. 20*, 105−123.
18. Kroemker, M., Rüdiger, A.-H., Jokusch, B. M., and Rüdiger, M (1994) *FEBS Lett. 355*, 259−256.
19. Pavalko, F. M., and Burridge K. (1991) *J. Cell. Biol. 114*, 481−491.
20. Smillie, L. B. (1982) *Methods Enzymol. 35*, 234−241.
21. Kauppinen, J. K., Moffat, D. J., and Mantsch, H. H. (1981) *Appl. Spectrosc. 35*, 271−276.
22. Kauppinen, J. K., Moffat, D. J., Mantsch, H. H., and Cameron, D. G. (1981) *Anal. Chem. 53*, 1454−1457.
23. Byler, D. M., and Susi, H. (1986) *Biopolymers 25*, 469−487.
24. Chirgadze, Yu. N., Fedorov, O. V., and Trushina, N. P. (1975) *Biopolymers 14*, 679−694
25. Venyaminov, S. Yu., and Kalnin, N. N. (1990) *Biopolymers 30*, 1243−1257
26. Venyaminov, S. Yu., and Kalnin, N. N. (1990) *Biopolymers 30*, 1259−1271
27. Blundell, T., Barlow, D., Borkakoti, N., and Thornton, J. (1983) *Nature 306*, 281−283.
28. Saudek, V., Pastore, A., Castiliglione Morelli, M. A., Frank, R., Gausepohl, H., Gibson, T., and Roesch, P. (1990) *Protein Eng. 4*, 3−10.
29. Pascual, J., Pfuhl, M., Walther, D., Saraste, M., and Nilges, M. (1997) *J. Mol. Biol. 273*, 740−751.
30. Krimm, S., and Bandekar, J. (1986) *Adv. Protein Chem. 38*, 181−364.
31. Gonzales, L., Jr., Brown, R. A., Richardson, D., and Alber, T. (1996) *Nature New Biol. 3*, 1002−1010.

32. O'Shea, E. K., Rutkowski, R., andKim, P. S. (1992) *Cell 68*, 699−708.
33. Lilias, A., and Rossmann, M. (1974) *Annu. Rev. Biochem 43*, 480−507.
34. Pauling, L., and Corey, R. B. (1953) *Nature 171*, 59−61.
35. Junius, F. K, Weiss, A. S., and King, G. F. (1993) *Eur. J. Biochem. 214*, 45−424.
36. Goodman, E. M., and Kim, P. S. (1991) *Biochemistry 30*, 11615−11620.
37. Trewhella, J., Liddle. W. K., Heidorn, D.B., and Strynadka, N. (1989) *Biochemistry 28*, 1294−1301
38. Jackson, M., Haris, P. I., and Chapman, D.(1991) *Biochemistry 30*, 9681−9686
39. Parrish, J. R., and Blout, E. R. (1972) *Biopolymers 11*, 1001−1020
40. . Reisdorf, W. C., and Krimm, S. (1994) *Biophys. J.*65, A373
41. Krimm, S., and Dwivedi, A. M. (1982) *Science 216*, 407−408
42. Tamm, L. K., and Tatulian, S. A. (1997) *Quart. Rev. Biophys.30*, 365−429
43. Bauer, H. H., Müller, M., Goette, J., Merkle, H. P., and Fringeli, U. P. (1994) *Biochemistry 33*, 12276−12282
44. Martinez, G., and Millhauser, G. (1995) *J. Struct. Biol. 114*, 23−27
45. Shaw, R. A., Buchko, G. W., Wang, G., Rozek, A., Treleaven, W. D. Mantsch, H. H., and Cushley, R. J. (1997) *Biochemistry 36*, 14531−14538
46. Harbury, P. B., Kim, P. S., and Alber, T. (1994) *Nature. 371*, 80−83

BI983079H